東北大学機関リポジトリ
TOUR
Tohoku University Repository

# BER analysis of convolution coded QDPSK in digital mobile radio



| | |
|---|---|
| 著者 | 安達　文幸 |
| journal or publication title | IEEE Transactions on Vehicular Technology |
| volume | 40 |
| number | 2 |
| page range | 435-442 |
| year | 1991 |
| URL | http://hdl.handle.net/10097/46482 |


doi: 10.1109/25.289425

# BER Analysis of Convolution Coded QDPSK in Digital Mobile Radio

Tadashi Matsumoto, *Member, IEEE,* and Fumiyuki Adachi, *Senior Member, IEEE*

*Abstract*—**Bit error rate (BER) performance of convolutional coded quaternary DPSK (QDPSK) with Viterbi decoding is theoretically investigated in Rayleigh fading environments. The probability density functions of the path and branch metric values of Viterbi decoding are derived. The BER's after decoding due to additive white Gaussian noise (AWGN) and cochannel interference are theoretically analyzed. Rate 1/2 codes and their symbol punctured high-rate codes are considered, and the optimal symbol positions for deletion to minimize the BER after decoding are presented for the codes with constraint length $K = 3$–7. It is shown that Viterbi decoding considerably reduces the desired signal-to-interference power ratio (SIR), as well as the signal energy per information bit-to-noise power spectrum density ration $(E_b/N_0)$, necessary to achieve a certain BER. The spectrum efficiency of the cellular mobile radio system, achievable by the use of the symbol punctured codes, is also evaluated.**

## I. Introduction

In land mobile radio, the received signal is subjected to fast multipath fading caused by reflections from obstacles near the mobile station [1]. If a relatively low bit rate signal (lower than say 64 kb/s), whose bandwidth is smaller than the coherence bandwidth of a multipath channel, is transmitted, the major causes of errors are envelope variation and random FM noise of the received signal due to multipath fading [2]. Random FM noise (or random phase noise) places a lower limit on the achievable bit error rate (BER). In a cellular system, the same radio frequency is reused in spatially separated cells in order to use effectively the limited resources of available frequency spectra. Cochannel interference performance determines the spatial utilization of the radio spectrum. However, under multipath fading, cochannel interference performance is severely degraded.

A well-known technique to reduce the effect of fading is diversity reception [3], [4, chap. 10]. Postdetection diversity reception has been proposed and extensively studied for continuous phase modulation (CPM) and quaternary DPSK (QDPSK) [5], [6]. Another attractive technique is forward error correction (FEC). Convolutional codes using Viterbi decoding have powerful error correction capability. Although many previous papers [7], [8] have been devoted to the BER performance analysis of convolutional codes under additive white Gaussian noise (AWGN) and Rayleigh fading, no analysis has been reported for their BER performance taking co-channel interference and random FM noise into consideration.

Manuscript received February 6. 1990; revised May 7, 1990 and November 1, 1990. This paper was presented at the Symposium on Information Theory and Its Application (SITA'89), Inuyama, Japan, December 1989.

The authors are with the NTT Radio Communication Systems Laboratories, Yokosuka 238, Japan.

IEEE Log Number 9144309.

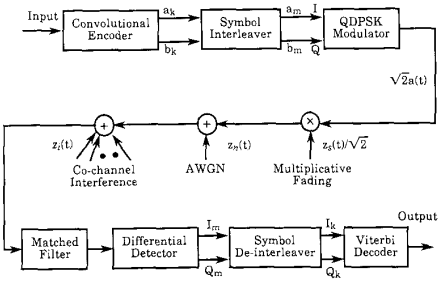


Fig. 1. Complex representation of system model.

This paper investigates the BER performances of linear convolutional coded QDPSK with Viterbi decoding in multiplicative Rayleigh fading channels. A QDPSK signal can be detected either by a differential detector or a coherent detector with differential decoding. Since differential detection requires no carrier recovery function, it is thus promising for mobile radio applications (coherent detection is difficult to use because of fast variations in the received signal phase due to fading). In this paper, differential detection is assumed. The system model used in the analysis is presented for rate 1/2 convolutional codes in Section II. The method of obtaining branch and path metric values, and the mathematical expression for their probability density functions (PDF's) are described in Section III. Then, the average BER after decoding is calculated for fast Rayleigh fading taking into account both AWGN and cochannel interference. The BER performances of convolutional codes with rates higher than 1/2, which are derived from the rate 1/2 codes by a symbol puncturing technique, are calculated and shown in Section IV. The spectrum efficiency of a cellular mobile system achievable by using the symbol punctured high rate codes is investigated in Section V.

## II. System Model

The block diagram of the system under investigation is shown in Fig.1. The input bit stream is encoded by a rate 1/2 linear convolutional coder whose output symbols $(a_k, b_k)$ are then block-interleaved symbol-by-symbol, where $k$ is an integer. It is assumed that the interleaving degree is large enough to randomize the burst errors produced by Rayleigh fading.

The symbol sequence after interleaving is denoted by $(a_m, b_m)$, where $m$ is an integer. The signal space diagram of QDPSK is shown in Fig. 2. The QDPSK signal $e(t)$ to be

0018-9545/91/0500-0435$01.00 © 1991 IEEE

Authorized licensed use limited to: TOHOKU UNIVERSITY. Downloaded on March 05,2010 at 02:18:41 EST from IEEE Xplore. Restrictions apply.

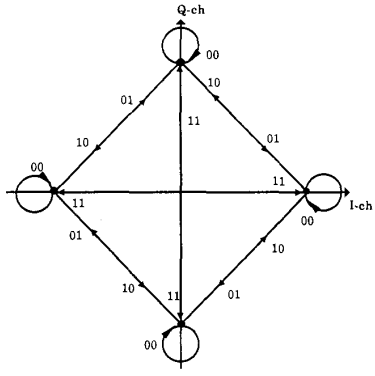


Fig. 2. Signal space diagram of QDPSK.

transmitted is, with a unit power,

$$e(t) = \mathrm{Re}\left\{\sqrt{2}\,a(t)e^{j\omega_c t}\right\} \tag{1}$$

where $\mathrm{Re}(\cdot)$ is the real part of the complex value, $\omega_c$ is the carrier angular frequency, and

$$a(t) = \exp\left[j\sum_{m=-\infty}^{\infty}\Phi_m g(t-mT)\right] \tag{2}$$

with $\Phi_m \in \{0, \pi/2, \pi, 3\pi/2\}$ being the $m$th phase and $g(t)$ a unit pulse of duration $T$ centered at $t = 0$. The transmitted symbol $(a_m, b_m)$ is "mapped" to the phase difference $\Delta\Phi_m = (\Phi_m - \Phi_{m-1}) \bmod 2\pi$ in the QDPSK modulator. The mapping rule considered in this paper is given by

$$\Delta\Phi_m = \begin{cases} 0, & (a_m, b_m) = (-1, -1) \\ \pi/2, & (a_m, b_m) = (+1, -1) \\ \pi, & (a_m, b_m) = (+1, +1) \\ 3\pi/2, & (a_m, b_m) = (-1, +1). \end{cases} \tag{3}$$

The transmitted QDPSK signal is received via the Rayleigh fading channel and is differentially detected. The sampled values of the detector output are then de-interleaved, and fed to the Viterbi decoder.

## III. BER Analysis for Rate 1/2 Codes

### A. Mathematical Representation of Detector Output

Both the desired signal and cochannel interference are assumed to have a bandwidth less then the coherence bandwidth of the multipath channel. The received signal is then subjected to multiplicative fading. We also assume that the fading is very slow compared to the symbol rate $1/T$. The complex envelope $z(t)$ of the matched filter output can be represented as

$$z(t) = z_s(t)a(t) + z_i(t) + z_n(t) \tag{4}$$

where subscripts $s$, $i$, and $n$ denote the desired signal, cochannel interference and bandlimited AWGN, respectively. Assume the Rayleigh fading, $z_s(t)$ and $z_i(t)$, are mutually independent zero-mean complex Gaussian processes with average powers of $\sigma_s^2$ and $\sigma_i^2$, respectively. The average power of $z_n(t)$ is given by $N_0/T$, where $N_0$ is the *single-sided noise power spectrum density*. Strictly speaking, the statistical property of faded cochannel interference is affected by the modulating symbol sequence. However, in this paper we assume that the cochannel interference is unmodulated because most of the errors are produced by Rayleigh fading itself rather than the modulating sequence, and thus it can be treated as complex Gaussian noise. On the other hand, if many modulated interference sources are considered, the composite interference component approaches complex Gaussian process according to the central limit theorem. This assumption allows for considerable simplification of the analysis.

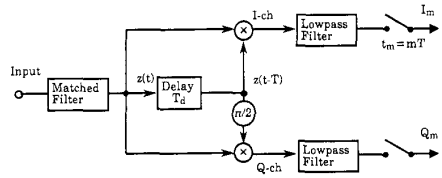


Fig. 3. Quadrature differential detector.

The QDPSK signal is detected by the differential detector illustrated in Fig. 3, where $\omega_c T_d \bmod 2\pi = -\pi/4$ and $T_d \approx T$. The I-ch and Q-ch outputs $I(t)$ and $Q(t)$ are then sampled at $t_m = mT$, and are expressed in the complex form as

$$I_m + jQ_m = z_m \cdot z_{m-1}^* e^{j\pi/4} \tag{5}$$

where $i_m = I(mT)$, $Q_m = Q(mT)$, $z_m = z(mT)$, and $*$ denotes the complex conjugate.

After de-interleaving, the sample sequence of $I_k = I(kT)$ and $Q_k = Q(kT)$ is obtained. Without noise and cochannel interference, the de-interleaver output is

$$I_k + jQ_k = z_{s,k} \cdot z_{s,k-1}^* e^{j(\Delta\Phi_k + \pi/4)} \tag{6}$$

where $z_{s,k} = z_s(kT)$. Since $\exp\{j(\Delta\Phi_k + \pi/4)\} = a_k + jb_k$, the decision on the transmitted di-bit symbol can be independently made based on the polarity of $I_k$ and $Q_k$ for hard decision decoding.

### B. Branch and Path Metric

The Viterbi decoder calculates the $k$th branch metric $L_k$ from samples $I_k$ and $Q_k$. For differential detection, the most practical choice for branch metric, which is not the maximum likelihood metric, is [9]

$$L_k = -\mathrm{Re}\left[(a_k' + jb_k')(I_k + jQ_k)^*\right] = -a_k' I_k - b_k' Q_k \tag{7}$$

where $(a_k', b_k') = (\pm 1, \pm 1)$ is the $k$th symbol in a possible sequence. This branch metric is similar to that for coherent detection except that $I_k$ and $Q_k$ are non-Gaussian variables.

The path metric is the sum of the branch metric values along the path, $l = \Sigma L_k$. The Viterbi decoder compares the path metric values of the possible paths, and selects the symbol sequence with the greatest path metric value at each path merger. Erroneous decoding results from incorrect path survival. The probability that an incorrect path is selected can be calculated from the PDF of the path metric.

Let us assume that the convolutional code has a codeword $X_0$ with an all-zero symbol sequence which corresponds to

Authorized licensed use limited to: TOHOKU UNIVERSITY. Downloaded on March 05,2010 at 02:18:41 EST from IEEE Xplore. Restrictions apply.

all $(a_k, b_k) = (-1, -1)$. We also assume for the calculation of the average BER after decoding that the codeword $X_0$ is transmitted without loss of generality, because the linear property of the distance structure of the convolutional code is retained by the mapping rule shown in Fig. 2. The codeword $X_0$ corresponds to the all-zero state path in the trellis diagram. Consider the opposing codeword $X_{di}$ with length $d$, whose path diverges from $X_0$'s all-zero state path and merges with it after $d$ steps. The transmitted codeword $X_0$ survives if $l_0 \geqq l_{di}$ where $l_0$ and $l_{di}$ are the path metric values of $X_0$ and $X_{di}$, respectively. Otherwise, the opposing codeword $X_{di}$ survives. Let the number of the symbol (1, 1) in $X_{di}$ be denoted by $L$. Furthermore, let the numbers of the symbols (1, −1) and (−1, 1) in $X_{di}$ be denoted by $M$ and $N$, respectively. Note that $L + M + N +$ {the number of the symbol $(-1, -1)$ in $X_{di}$} $= d$. Note further that the smallest $L + M + N$ value is the length of the shortest error event path defined by Divslar and Simon [10]. Let $l_0'$ be given as

$$l_0' = \sum_{(a_k', b_k')=(1,1)} (I_k + Q_k) + \sum_{(a_k', b_k')=(1,-1)} I_k + \sum_{(a_k', b_k')=(-1,1)} Q_k. \quad (8)$$

Obviously, $l_0 \geqq l_{di}$ is equivalent to $l_0' \geqq 0$.

### C. Average BER

The average BER $P_b$ after decoding is upper bounded by

$$P_b \leqq \sum_{d=K}^{\infty} \sum_{i=1}^{N_d} n_{di} P_{di} \quad (9)$$

where $n_{di}$ is the number of the error bits produced in the Viterbi decoder output when the opposing codeword $X_{di}$ is selected, $P_{di}$ is the average probability that the opposing codeword $X_{di}$ survives (this happens if $l_0' < 0$), $N_d$ is the number of all possible opposing paths with length $d$, and $K$ is the constraint length of the code. The infinite sum in (9) with respect to $d$ can be approximated by the sum of several finite terms because the average survival probability $P_{di}$ for the opposing codeword having the smallest $L + M + N$ value becomes dominant term (this is shown in the later part of this section). The codewords with the smallest $L + M + N$ value appear among the codewords with small $d$ values.

It can be observed from (8) that the value $l_0'$ is equivalent to postdetection diversity combiner output with $L + M + N$ branches. Therefore, the process of Viterbi decoding can be viewed as postdetection diversity reception (this was suggested by Simon and Divslar [10]). Postdetection diversity reception combines all branch outputs after detection. The derivation method for the BER proposed by Adachi and Parsons [5] can be applied here. The method makes it possible to calculate the BER due to AWGN, random FM noise, and cochannel interference in Rayleigh fading.

*1) Average Survival Probability $P_{di}$:* The conditional PDF, $p\{z_{k-1}^* \mid z_k\}$, of $z_{k-1}^*$ with $z_k$ being given is given by [5]

$$p\{z_{k-1}^* \mid z_k\} = \frac{1}{2\pi\sigma^2(1 - |\mu|^2)} \cdot \exp\left\{\frac{-|z_{k-1} - \mu^* z_k|^2}{2\sigma^2(1 - |\mu|^2)}\right\} \quad (10)$$

where $\sigma^2 = 1/2 < |z_k|^2 > = 1/2 < |z_{k-1}|^2 >$, $\mu = \mu_{re} + j\mu_{im} = 1/2 < z_k \cdot z_{k-1}^* > /\sigma^2$. Equation (10) shows that with $z_k$ given, $z_{k-1}$ is a complex Gaussian variable with mean $\mu^* z_k$ and variance $\sigma^2(1 - |\mu|^2)$. Therefore, $I_k$ and $Q_k$ become independent Gaussian variable. The mean values are $\mu_{re}|z_k|^2$ for $I_k$ and $\mu_{im}|z_k|^2$ for $Q_k$. The variance value is $\sigma^2(1 - |\mu|^2)|z_k|^2$ for both $I_k$ and $Q_k$. The autocorrelation $\mu$ is given by [5]

$$\mu = \mu_s \frac{\Gamma}{\Gamma(1 + 1/\Lambda) + 1} \cdot \frac{(1 + j)}{\sqrt{2}} \quad (11)$$

where $\mu_s = 1/2 < z_{s,k} \cdot z_{s,k-1}^* > /1/2 < |z_{s,k}|^2 >$ is the autocorrelation at a time displacement of $T$ of the fading complex envelope $z_s(t)$ for the desired signal, $\Gamma = \sigma_s^2 T/N_0$ is the average *signal energy per symbol-to-noise power spectral density ratio* $(E_s/N_0)$, and $\Lambda = \sigma_s^2/\sigma_i^2$ is the average *signal-to-interference power ratio* (SIR).

Since we assume perfect symbol interleaving, all $(I_k + jQ_k)$'s are statistically independent. From the above discussion, if all $z_k$'s are conditioned at symbol positions where the opposing codeword $X_d$ has different symbols from $X_0$, the value $l_0'$ also becomes a random variable with mean

$$(\mu_{re} + \mu_{im}) \sum_{(a_k', b_k')=(1,1)} |z_k|^2 + \mu_{re} \sum_{(a_k', b_k')=(1,-1)} |z_k|^2 + \mu_{im} \sum_{(a_k', b_k')=(-1,1)} |z_k|^2$$

and variance

$$\sigma^2(1-|\mu|^2)\left(2\sum_{(a_k', b_k')=(1,1)} |z_k|^2 + \sum_{(a_k', b_k')=(1,-1)} |z_k|^2 + \sum_{(a_k', b_k')=(-1,1)} |z_k|^2\right).$$

Therefore, the conditional probability $p_{di}$ that the opposing codeword $X_{di}$ survives is given by

$$R_0 = \frac{1}{2}\operatorname{erfc}\left[\frac{(\mu_{re} + \mu_{im}) \sum_{(a_k', b_k')=(1,1)} |z_k|^2 + \mu_{re} \sum_{(a_k', b_k')=(1,-1)} |z_k|^2 + \mu_{im} \sum_{(a_k', b_k')=(-1,1)} |z_k|^2}{\sqrt{2\sigma^2(1 - |\mu|^2)\left(2\sum_{(a_k', b_k')=(1,1)} |z_k|^2 + \sum_{(a_k', b_k')=(1,-1)} |z_k|^2 + \sum_{(a_k', b_k')=(-1,1)} |z_k|^2\right)}}\right] \quad (12)$$

where erfc $(\cdot)$ is the complementary error function.

If the autocorrelation $\mu_s$ of the fading complex envelope is a real function (this happens when $z_s(t)$ has a symmetric

Authorized licensed use limited to: TOHOKU UNIVERSITY. Downloaded on March 05,2010 at 02:18:41 EST from IEEE Xplore. Restrictions apply.

power spectrum), $\mu_{re} = \mu_{im}$. Then, (12) can be simplified to

$$p_{di} = \frac{1}{2}\operatorname{erfc}\left[\frac{\mu_{re} R_0}{\sqrt{2\sigma^2(1 - |\mu|^2)}}\right] \tag{13}$$

where

$$R_0 = \sqrt{2\sum_{(a'_k, b'_k)=(1,1)} |z_k|^2 + \sum_{(a'_k, b'_k)=(1,-1)} |z_k|^2 + \sum_{(a'_k, b'_k)=(-1,1)} |z_k|^2}. \tag{14}$$

The average survival probability $P_{di}$ can be obtained by averaging (13) over the PDF of $R_0$. Since we are assuming that all $z_k$'s are statistically independent, the characteristic function approach can be applied for the derivation of the PDF of $R_0$. The characteristic function $C(s)$ of $R_0^2/2$ is given by

$$C(s) = \frac{1}{(1 - s\sigma^2 s)^L \cdot (1 - \sigma^2 s)^{M+N}}. \tag{15}$$

The PDF of $R_0^2/2$ is derived using the inverse Laplace transform of $C(s)$, and finally we obtain the PDF of $R_0$ using $p(R_0) = R_0 \cdot p(R_0^2/2)$. Let the Laurent series expansion of the characteristic function $C(s)$ of $R_0^2/2$ be denoted as

$$C(s) = \sum_{j=L+M+N}^{\infty} \alpha_j s^{-j} \tag{16}$$

where $\alpha_j$'s are the residues of $C(s)$. The PDF $p(R_0)$ can be expressed as

$$p(R_0) = \sum_{j=L+M+N}^{\infty} a_j \frac{R_0^{2j-1}}{2^{j-1}(j-1)!}. \tag{17}$$

The first two residues $\alpha_{L+M+N}$ and $\alpha_{L+M+N+1}$ are given by

$$\alpha_{L+M+N} = 1/(2^L \sigma^{2(L+M+N)}) \tag{18}$$

$$\alpha_{L+M+N+1} = -(M + N + L/2)\alpha_{L+M+N}/\sigma^2. \tag{19}$$

Averaging the conditional survival probability given by (13) using (17), we obtain the average survival probability $P_{di}$ as

$$P_{di} = \frac{1}{2}\sum_{j=L+M+N}^{\infty} a_j \sigma^{2j} \frac{(2j-1)!!}{j!}\left\{\frac{\sqrt{(1 - |\mu|^2)}}{\sqrt{2}\,\mu_{re}}\right\}^{2j}. \tag{20}$$

Substituting (11) into (20) yields $P_{di} \propto \Gamma^{-(L+M+N)}$ and $P_{di} \propto \Lambda^{-(L+M+N)}$ for large $\Gamma$ and $\Lambda$. Therefore, the important point to be noted is that the parameter which dominates the survival probability $P_{di}$ is the value $L + M + N$. Also, it is found from (18)–(20) that $P_{di} \propto 2^{-L}$. It is apparent that, for QDPSK, $2^L = \Pi_{(a'_k, b'_k)\neq(-1,-1)}(1 - \cos\Delta\Phi_k)$ is the product of the squared branch distance. Thus the design criteria for minimizing the BER after decoding is *to maximize the length of the shortest error event path* (*maximize the smallest* $L + M + N$ *value*) and *the product of the squared branch distances*. This thoroughly agrees with the result of Divsalar and Simon [10] obtained through the Chernoff-bound approach.

The optimal code derived through the design criteria achieves the best performances among the codes with the same constraint length. However, it is difficult to evaluate coding gains with the Chernoff-bound approach because of its looseness [14]. The upper bound of the BER derived in this paper is tighter than that derived through the Chernoff-bound approach because no approximation was used in the derivation process for the average survival probability given by (20). The approximation that only the first few residues are used for the calculation of (20) is tight for large $\Gamma$ and $\Lambda$ because the first term in (20) dominates the survival probability. Therefore, the approach described in this paper makes it possible to evaluate the coding gains achieved by the optimal codes. Furthermore, another attractive feature of this approach is that the cochannel interference performance can be derived. This allows us to evaluate the spectrum efficiencies of cellular systems employing the optimal codes. Evaluated coding gains and spectrum efficiencies are presented in Sections IV and V.

### D. Calculation Results

The BER performances of several convolutional codes are calculated using the first two residues $\alpha_{L+M+N}$ and $\alpha_{L+M+N+1}$ given by (18) and (19). Assuming that equal amplitude multipath waves arrive from all directions with equal probability, $\mu_s(T) = J_0(2\pi f_D T)$ [2, pp. 19–39], where $J(\cdot)$ is the zeroth-order Bessel function and $f_D$ is the maximum Doppler frequency given by *vehicle speed/carrier wavelength*. For example, $f_D = 40$ Hz when the vehicle speed is 48 km/h at a carrier frequency of 900 MHz.

The generator polynomials [11] of the codes used for the calculation are shown in Table I. The BER's of the codes having the same length of the shortest error event path are distinguished by the total information weight $\Sigma n_{di}$ along all the shortest paths. The shortest error event path length and the total information weight are listed in the table. The average BER's after decoding versus *signal energy per information bit-to-noise power spectrum density ratio* $E_b/N_0 (= E_s/N_0$ for rate 1/2 codes) are shown in Fig. 4(a) for SIR = 20 dB and in Fig. 4 (b) for SIR $\rightarrow \infty$ with the parameter of constraint length $K$. $f_D T \rightarrow 0$ is assumed (this corresponds to very slow Rayleigh fading). As the constraint length $K$ increases, the improvement in average BER becomes larger.

Coding gain is defined as the reduction in $E_b/N_0$ necessary to obtain a certain BER. The results are plotted in Fig. 5

Authorized licensed use limited to: TOHOKU UNIVERSITY. Downloaded on March 05,2010 at 02:18:41 EST from IEEE Xplore. Restrictions apply.

TABLE I
GENERATOR POLYNOMIALS

| $K$ | Generator polynomials (octal) | Shortest error event path length (information weight) |
|---|---|---|
| 3 | 5 | 3(1) |
| | 7 | |
| 4 | 15 | 4(3) |
| | 17 | |
| 5 | 23 | 5(6) |
| | 35 | |
| 6 | 53 | 6(5) |
| | 75 | |
| 7 | 133 | 6(1) |
| | 171 | |

at BER = $10^{-4}$ for $f_DT \to 0$ and SIR $\to \infty$. The coding gain increases from 21.5 to 26 dB as $K$ increases from 3 to 7.

The average BER performance as a function of SIR is also shown in Fig. 4 for $f_DT \to 0$. It is found from these figures that the SIR necessary to achieve a certain BER is considerably reduced by coding.

For slow Rayleigh fading, errors are mainly caused by AWGN and cochannel interference. For fast Rayleigh fading, however, most errors tend to be produced by random FM noise as the average $E_b/N_0$ and SIR increase. The random FM noise places a lower limit on achievable BER. The average BER after decoding versus $f_DT$ with $\Lambda$ as parameter when $\Gamma \to \infty$ (or with $\Gamma$ as parameter when $\Lambda \to \infty$) is shown in Fig. 6(a). The BER floor is due to cochannel interference (AWGN) for $f_DT \leq 10^{-2}$, and is due to random FM noise for $f_DT > 10^{-2}$, when $\Lambda$ = 20dB. The average BER due to random FM noise versus $f_DT$ is shown in Fig. 6(b). The BER can be made negligibly small by coding (order of $10^{-15}$ for $f_DT = 10^{-3}$ even when a code with $K = 3$ is used).

## IV. SYMBOL PUNCTURED CODES

In the previous section, we assumed rate 1/2 convolutional codes. However, for a given channel bandwidth, FEC codes with rates higher than 1/2 are required to achieve higher bit rate transmission. A simple and attractive method to produce high-rate codes is the puncturing technique. The high-rate codes are obtained by periodically deleting some bits from rate 1/2 (or lower) convolutional coder output. The optimal bit positions for deletion to minimize the BER after decoding have been found in AWGN channels (no fading) through computer-search for the original rate 1/2 convolutional codes with the constraint length $K$ = 3–9 [11]. However, no performance analysis for the punctured convolutional codes have been reported in fading channels.

If we apply bit puncturing to the convolutional coded QDPSK system with symbol interleaving described in Section II, the one-to-one mapping rule between the branch symbol and the MDPSK symbol is no longer retained. Therefore, it is reasonable to restrict our investigation within symbol punctured codes.

The procedure for constructing the symbol punctured convolutional codes is shown in Fig. 7. $p - 1$ symbols (i.e., $2p - 2$ bits) among $2p$ symbols (i.e., $4p$ bits) of the original code sequence are periodically deleted (this $2p$-symbol interval is referred to as the puncturing period in this paper for convenience), according to the deleting map, to produce rate $p/(p + 1)$ code. The average BER is upper

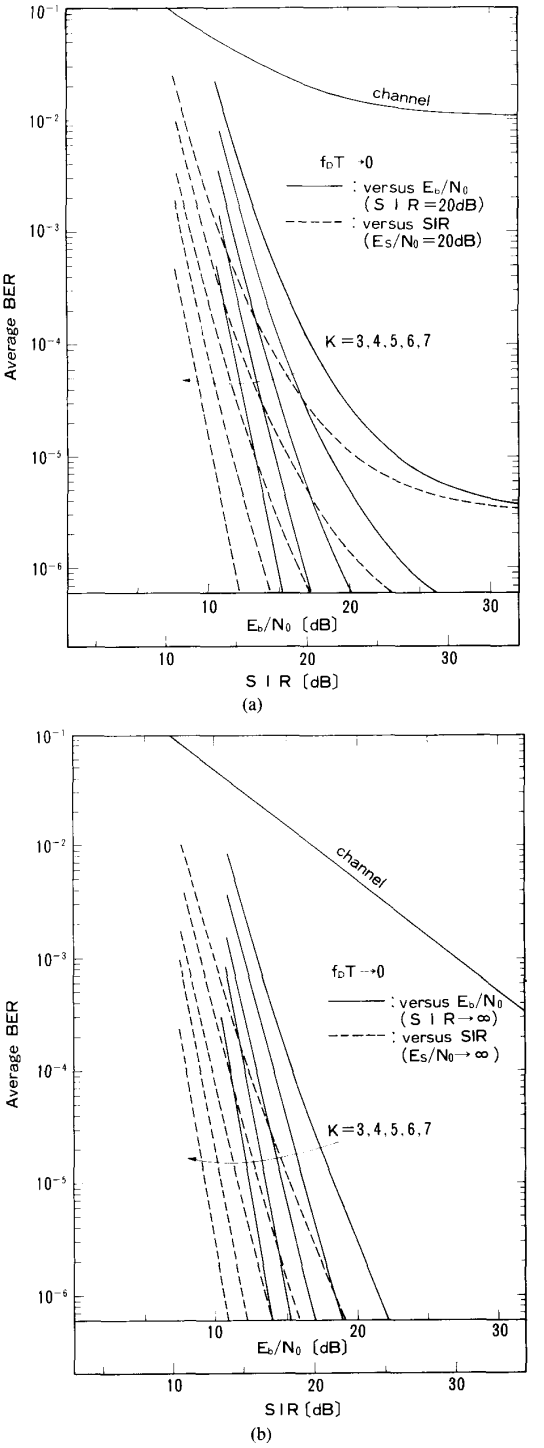


Fig. 4. BER versus $E_b/N_0$ (or SIR) for $f_Dt \to 0$. (a) SIR = 20 dB (or $E_s/N_0$ = 20 dB). (b) SIR $\to \infty$ (or $E_s/N_0 \to \infty$).

Authorized licensed use limited to: TOHOKU UNIVERSITY. Downloaded on March 05,2010 at 02:18:41 EST from IEEE Xplore. Restrictions apply.

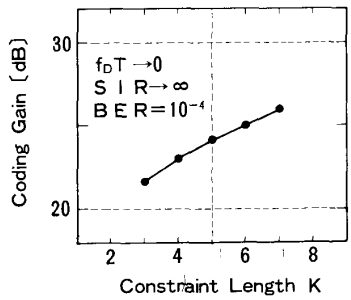


Fig. 5. Coding gain at BER = $10^{-4}$ for $f_DT \to 0$.

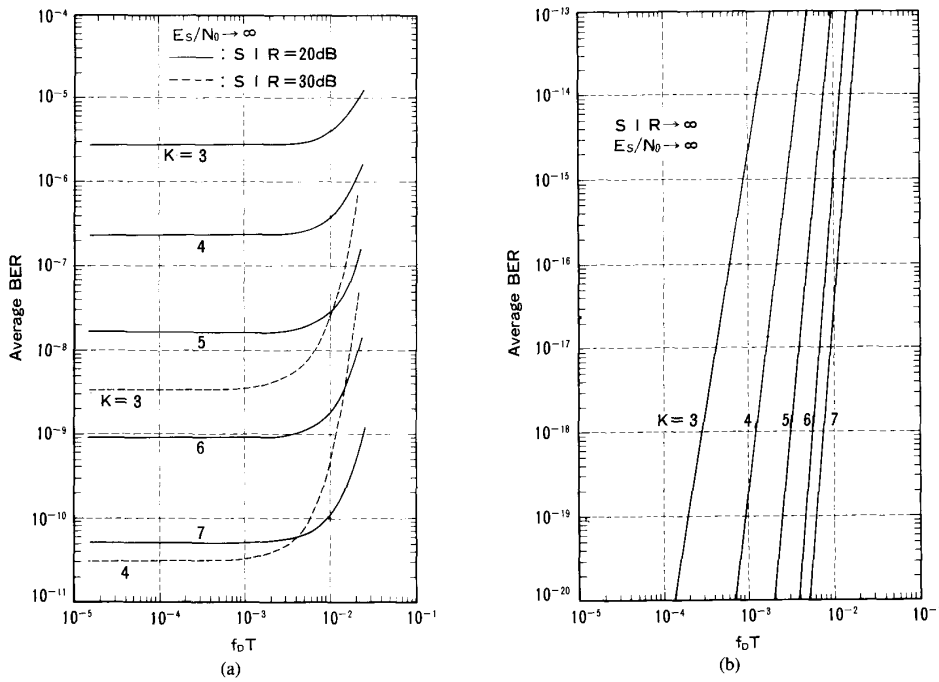


Fig. 6. BER after decoding. (a) SIR = 20 and 30 dB, and $E_s/N_0 \to \infty$ (or $E_s/N_0$ = 20 and 30 dB, and SIR $\to \infty$). (b) $E_s/N_0 \to \infty$ and SIR $\to \infty$).

bound by

$$p_b \leqq \frac{1}{2p} \sum_{d=K}^{\infty} \sum_{i=1}^{N_d'} n_{di} P_{di} \tag{21}$$

where $N_d'$ is the number of all the possible opposing paths with length $d$, which diverge from the all-zero state path during the puncturing period.

*2) Optimal Symbol Punctured Codes and their Coding Gains:* The optimal deleted symbol positions to minimize the BER after decoding were computer-searched for $p$ = 2–6. The rate 1/2 convolutional codes shown in Table I were used as the original codes. In the search process, symbol punctured codes having the maximum value of the shortest error event path length were first picked as candidates for the given $K$ and $p$. Then, the code which achieved the lowest BER after decoding was found from the candidate codes (BER was calculated using (21) for each of the candidates).

The search results for the optimal symbol position are presented in Table II. The shortest error event path length and the total information weight $\Sigma n_{di}$ of these punctured codes are also listed. Of course, these codes were checked to verify that they were noncatastrophic. An interesting point to be noted from this table is that all of the original codes have the same deleted symbol positions for optimal puncturing except for the $K$ = 4 rate 4/5 code.

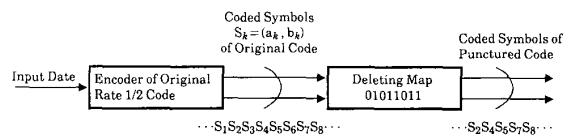


Fig. 7. Procedure for constructing symbol punctured codes (for example, $p$ = 4).

The coding gains at BER = $10^{-4}$ versus code rate are plotted in Fig. 8 for $f_DT \to 0$ and SIR $\to \infty$ with constraint length $K$ as a parameter. For all codes, a rapid decrease in the coding gain is observed when the rate increases from 1/2

Authorized licensed use limited to: TOHOKU UNIVERSITY. Downloaded on March 05,2010 at 02:18:41 EST from IEEE Xplore. Restrictions apply.

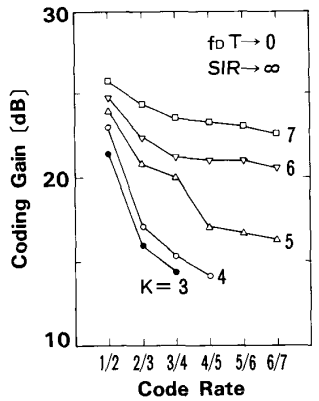


Fig. 8. Coding gains at BER = $10^{-4}$ versus code rate for symbol punctured codes.

TABLE II
OPTIMAL POSITIONS FOR SYMBOL DELETION, THE SHORTEST ERROR EVENT PATH LENGTH, AND INFORMATION WEIGHT ALONG ALL THE SHORTEST PATHS

| | | Rate | | | | |
|---|---|---|---|---|---|---|
| | $K$ | 2/3 | 3/4 | 4/5 | 5/6 | 6/7 |
| Symbol position | 4 | 0111 | 011011 | 01101011 | 0101101101 | 010101011011 |
| | 3, 5, 6, 7 | 0111 | 011011 | 01010111 | 0101101101 | 010101011011 |
| Shortest error event path length (information weight) | 3 | 2(5) | 2(24) | — | — | — |
| | 4 | 2(2) | 2(12) | 2(46) | — | — |
| | 5 | 3(13) | 3(86) | 2(11) | 2(36) | 2(47) |
| | 6 | 3(4) | 3(18) | 3(44) | 3(66) | 3(114) |
| | 7 | 4(12) | 3(10) | 3(33) | 3(57) | 3(108) |

Symbols whose positions are indicated as "1" are to be transmitted, and as "0" are to be deleted. Codes denoted by "—" have the shortest error event path length of 1 (offer no advantage).

to 2/3. Also, for the $K = 5$ code, the coding gain rapidly decreases when the rate increases from 3/4 to 4/5. These decreases are because of decrements in the shortest error event path length (see Tables I and II). A coding gain of about 23 dB remains for $K = 7$ codes even when the code rate increases from 3/4 to 6/7, because these symbol punctured codes have the same shortest error event path length. A similar feature can be seen for the $K = 6$ codes.

## V. SPECTRUM EFFICIENCY

In cellular mobile radio systems, improving the spectrum efficiency is an important issue because of the limited radio spectrum. The spectrum efficiency achievable with the symbol punctured high rate codes is given in this section. It has been shown [12] that the efficiency of a QPSK cellular mobile radio system with BCH coding tends to be insensitive to the code rate when diversity reception is used. As mentioned previously, Viterbi decoding can be viewed as postdetection diversity reception. Therefore, it is anticipated for the punctured high rate codes that the larger the shortest error event path length (equivalent to the number of diversity branches) becomes, the less sensitive to the code rate the spectrum efficiency tends to be.

The spectrum efficiency $\eta$ of a cellular system is defined as the product of three factors: in time, frequency, and space. When a rate $r$ code is used, the efficiency $\eta$ for a cellular system using a hexagonal cell layout can be represented as [12]

$$\eta \propto \frac{r}{\left\{1 + \left(\kappa \Lambda_{\text{th}}\right)^{1/\alpha}\right\}^2} \tag{22}$$

where $\alpha$ is the propagation constant (typical value is $\alpha = 3.5$) [2], [13], and $\kappa$ is the fading margin for the allowable probability $Q$ of geographical outage at the cell fringe due to shadow fading. Assuming log-normal shadow fading, $\kappa$ can be obtained from

$$Q = \frac{1}{2} \operatorname{erfc}\left\{\frac{\kappa}{2\delta}\right\} \tag{23}$$

where $\delta$ (in decibels) is the standard deviation of the shadow fading. $\Lambda_{\text{th}}$ is the average SIR necessary to achieve the specific BER after decoding when $E_s/N_0 \to \infty$. The value $\Lambda_{\text{th}}$ can be found from (9) for rate 1/2 codes and (21) for symbol-punctured codes.

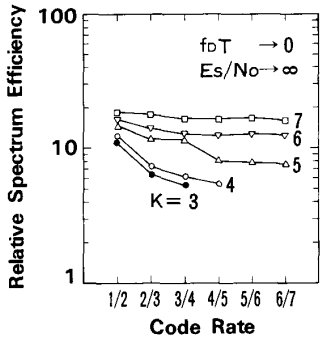


Fig. 9. Spectrum efficiency versus code rate of symbol punctured codes.

The calculated spectrum efficiencies in cellular mobile radios using the rate 1/2 and the symbol punctured high rate convolutional codes with $K = 3$–7 are shown in Fig. 9 for a required average BER after decoding of $10^{-4}$, $Q = 1\%$, $\alpha = 3.5$ and $\delta = 6$ dB. The efficiency is normalized by that with no coding. For the codes with $K = 6$ and $K = 7$, the spectrum efficiency is almost insensitive to the code rate. For the codes with $K = 3$ and $K = 4$, however, the efficiency decreases as the code rate increases, and the rate 3/4 code provides half the efficiency as achieved by the rate 1/2 code. These results are easily understood from the decrement property of the shortest error event path length shown in Tables I and II. For the codes with $K = 6$ and $K = 7$, the shortest error event path length remains 3 when the rate varies from 3/4 to 6/7.

Spectrum efficiency for the rate 6/7 code with $K = 6$ is roughly the same as that for the rate 1/2 code with $K = 4$. This implies that for a given channel bandwidth, the rate 6/7 code with $K = 6$ achieves an information transmission rate 12/7 times as high as that of the rate 1/2 code with $K = 4$, while keeping the spectrum efficiency constant. This is the advantage of using a high rate code with large $K$ in interference-limited environments.

## VI. CONCLUSION

BER performance of convolutional coded QDPSK with Viterbi decoding was investigated in Rayleigh-fading envi-

Authorized licensed use limited to: TOHOKU UNIVERSITY. Downloaded on March 05,2010 at 02:18:41 EST from IEEE Xplore. Restrictions apply.

ronments. The PDF's of the path and branch metric values for Viterbi decoding have been derived under a Rayleigh fading environment. The upper bound of BER's after decoding in AWGN and cochannel interference channels was analyzed using the derived PDFs for rate 1/2 codes and their symbol punctured high-rate codes. The optimal positions for symbol deletion to minimize BER after decoding were determined for the codes with constraint length $K = 3$–7. The coding gains of these codes were compared. It has been shown that Viterbi decoding considerably reduces SIR, as well as the $E_b/N_0$ necessary to achieve a certain BER. Also, the BER after decoding due to random FM noise was investigated. It has been shown that the BER due to random FM noise can be made negligibly small (order $10^{-15}$ for $f_D T = 10^{-3}$ by the rate 1/2 code with constraint length $K = 3$).

The spectrum efficiency of a cellular system, achievable with the optimal symbol punctured codes, was also investigated. It was shown that the efficiency is almost insensitive to the code rate for the codes with $K = 6$ and $K = 7$, while the efficiency of the rate 1/2 codes with $K = 3$ and $K = 4$ is roughly twice as large as that for the rate 3/4 codes.

If we use bit interleaving instead of symbol interleaving, we may locate the bit positions to be deleted so as to produce the best high rate codes which achieve the lowest BER in a fading channel. Performance analysis for bit puncturing in mobile radio environments is left as a further study.

## REFERENCES


[1] R. H. Clarke, "A statistical theory of mobile radio reception," *Bell Syst. Tech. J.*, vol. 47, pp. 957–1000, July 1968.

[2] W. C. Jakes, Jr., *Microwave Mobile Communications*. New York: Wiley, 1974.

[3] D. G. Brennan, "Linear diversity combining techniques," *Proc. IRE*, vol. 47, pp. 1075–1102, 1959.

[4] M. Schwartz, W. R. Benett, and S. Stein, *Communication Systems and Techniques*. New York: Wiley, 1974.

[5] F. Adachi and J. D. Parsons, "Error rate performance of digital FM mobile radio with postdetection diversity," *IEEE Trans. Commun.*, vol. COM-37, 3, pp. 200–209, 1988.

[6] K. Ohno and F. Adachi, "Postdetection diversity reception of QDPSK signals under frequency selective Rayleigh fading," in *Conf. Rec. IEEE VTC'90*, Orlando, FL, May 6–9, 1990.

[7] J. W. Modestino and S. Y. Mui, "Convolutional code performance in the Rician fading channel," *IEEE Trans. Commun.*, vol. COM-24, pp. 592–606, 1976.

[8] J. Hagenauer and E. Lutz, "Forward error correction coding for fading compensation in mobile satellite channels," *IEEE Trans. Select. Areas Commun.*, vol. SAC-5, pp. 215–225, 1987.

[9] D. Rainish and J. M. Perl, "Generalized cutoff rate of time- and frequency-selective fading channels," *IEEE Trans. Commun.*, vol. 37, pp. 449–467, 1989.

[10] D. Divsalar and M. K. Simon, "The design of trellis coded MPSK for fading channel: Performance criteria," *IEEE Trans. Commun.*, vol. 36, pp. 1004–1012, 1988.

[11] Y. Yasuda, K. Kashiki, and Y. Hirata, "High-rate punctured convolutional codes for soft decision Viterbi decoding," *IEEE Trans. Commun.*, vol. COM-32, pp. 315–319, 1984.

[12] F. Adachi and H. Suda, "Effects of diversity reception on BCH-coded QPSK cellular land mobile radio," *Electron. Lett.*, vol. 25, no. 3, pp. 188–189, 1989.

[13] Y. Okumura, E. Ohmori, T. Kawano, and K. Fukuda, "Field strength and its variability in VHF and UHF land mobile radio service," *Rev. Elec. Commun. Lab.*, no. 16, pp. 825–873, 1968.

[14] D. Divsalar and M. K. Simon, "Trellis coded modulation for 4800–9600 bits/s transmission over a fading mobile satellite channel," *IEEE Trans. Select. Area Commun.*, vol. SAC-5, pp. 162–175, 1987.


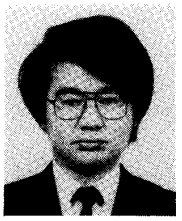

**Tadashi Matsumoto** (M'84) received the B.S. and M.S. degrees in electrical engineering in 1978 and 1980, respectively, and the Doctorate in engineering in 1991, all from Keio University, Yokohama-shi, Japan.

Since joining NTT in 1980, he participated in the R&D project of NTT's high capacity mobile communication system until 1987. Since May 1987, he has been researching digital mobile radio systems. His interest is in error control strategies such as FEC's and/or ARQ's in mobile radio channels. He is currently involved in the development of data communication systems for TDMA cellular mobile radios. He is a Senior Research Engineer of NTT Radio Communication Systems Laboratories, Yokosuka-shi.

Dr. Matsumoto is a member of the Institute of Electronics, Information and Communication Engineers of Japan.

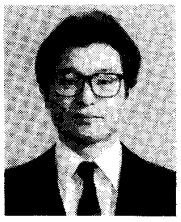

**Fumiyuki Adachi** (M'79–SM'90) graduated from Tohoku University, Japan, in 1973 and received the Engineering degree from the same University in 1984.

Since 1973 he has been with the Nippon Telegraph & Telephone Corporation (NTT) Laboratories, Japan, where his major activities included analytical and experimental works on diversity techniques for digital mobile radio communications. He was also concerned with man-made radio noise, syllabic compander for improving analog voice transmission quality, and statistical estimation of the signal strength in mobile radio. In addition to those activities, he contributed to the development of NTT analog cellular system with medium capacity. Currently he is a research group leader for mobile communication signal processing, including modulation/demodulation, diversity reception, channel coding, and is deeply involved in the development of TDMA cellular mobile radio system. During the academic year of 1984–1985, he was a U.K. SERC visiting research fellow at the Department of Electrical Engineering and Electronics of Liverpool University.

Dr. Adachi authored chapters in two books: Y. Okumura and M. Shinji, Eds., *Fundamentals of Mobile Communications* (in Japanese) (Japan: IEICE, 1986) and M. Shinji, Ed., *Mobile Communications* (in Japanese) (Japan: Maruzen, 1989). He was a co-organizer/chairman of the technical sessions for mobile/portable radio communications at IEEE GCOM'86–89. He also chaired the technical sessions at IEEE VTC'88 and '90. He was a member of the IEEE Communications Society Asian Pacific Committee from 1986 to 1989. He was a treasurer in 1989, and now is a secretary of the IEEE Vehicular Technology Society, Tokyo Chapter. He is a co-recipient the IEEE Vehicular Technology Society 1980 Paper of the Year Award. He is a member of the Institute of Electronics, Information, and Communication Engineers of Japan.

Authorized licensed use limited to: TOHOKU UNIVERSITY. Downloaded on March 05,2010 at 02:18:41 EST from IEEE Xplore. Restrictions apply.